Thyroid

DOI: 10.1089/thy.2016.0341

Thyroid
Low elasticity of thyroid nodules at ultrasound elastography is correlated with malignancy, degree of fibrosis and high expression of galectin-3 and fibronectin-1. (doi: 10.1089/thy.2016.0341)
This article has been peer-reviewed and accepted for publication, but has yet to undergo copyediting and proof correction. The final published version may differ from this proof.

Low elasticity of thyroid nodules on ultrasound elastography is correlated with malignancy, degree of fibrosis and high expression of galectin-3 and fibronectin-1.

Teresa Rago[1], Maria Scutari[1], Valeria Loiacono[1], Ferruccio Santini[1], Massimo Tonacchera[1], Liborio Torregrossa[2], Riccardo Giannini[2], Nicla Borrelli[2], Agnese Proietti [2], Fulvio Basolo[2], Paolo Miccoli[3], Paolo Piaggi[4], Francesco Latrofa[1], Paolo Vitti[1]

[1]Endocrinology Unit, University Hospital, [2]Department of Oncology Section of Cytopathology, Pathology, [13] Department of Surgery, [4]Department of Electric Systems and Automation, University of Pisa, Italy

*Abbreviated title***:** Thyroid Elastosonography and fibrosis

*Key words***:** Thyroid, thyroid ultrasound, US Elastography, Thyroid nodules, indeterminate cytology, fibrosis, Galectin-3, Fibronectin-1

Word Count : text: 3214 *;* abstract: 303

*Number of references***: 40**

*Number of Tables***: 4**

Number of Figures: 2

Corresponding Author: Teresa Rago M.D. Department of Clinical and Experimental Medicine, [1]Endocrinology Section, University of Pisa Via Paradisa, 2 56124 Pisa, Italy, Fax: +39 050/578772; Phone number: +39 050/997339; email: rago@endoc.med.unipi.it

*Disclosure Statment***:** the authors have nothing to disclose

Abstract

Background: Thyroid ultrasound elastography (US elastography) provides an estimation of tissue stiffness and is helpful to differentiate malignant from benign lesions. Tissue proprieties and molecules causing stiffness are not established. The aim of the study was to correlate US elastography findings with tissue properties in thyroid nodules.

Methods. 115 thyroid nodules from 112 patients who underwent surgery for the presence of of Thy 3 (indeterminate) cytology (n=67), Thy 4-5 (suspicious-indicative of carcinoma) cytology (n= 47) or large goiter in the presence of Thy 2 cytology (n= 1) and suspicious US features were examined by US elastography. Tissues obtained after surgery were characterized for cell number, microvessel density, fibrosis, expression of galectin-3 (Gal-3) and fibronectin-1(FN-1).

Results: Low elasticity on qualitative US elastography (LoEl) was found in 66 nodules, 1 benign and 65 carcinomas, high elasticity **(**HiEl) in 49 nodules, 46 benign and 3 carcinomas ($p<0.0001$). Quantitative analysis, performed in 24 nodules and expressed as elastic ratio between the strain of the nodule and that of the surrounding thyroid parenchyma, was 1.90 (1.18-2.77) (median and IQR) in 14 nodules with LoEl and 1.01-(0.91-1.10) in 10 nodules with HiEl ($p=0.002$). Stiffness did not correlate with cell number and was inversely correlated with microvessel density. Fibrosis was higher in nodules with LoEl than in those with HiEl ($p=0.009$) and in carcinomas than in benign nodules ($p=0.02$). Fibrosis was higher in nodules with high expression of Gal-3 ($p<0.001$) and FN-1 ($p=0.004$). Fibrosis and

expression of Gal-3 and FN-1 were higher in the classic vs the follicular variant of papillary thyroid carcinoma and lower in follicular adenomas.

Conclusions: i) Low elasticity at US elastography is highly correlated with malignancy; ii) nodule stiffness is correlated with fibrosis and expression of Gal-3 and FN-1; iii) these features are more evident in the classic than in the follicular variant of papillary thyroid carcinoma.

Introduction

Nodular thyroid disease is a common finding in the general population, in particular in iodine deficient areas. Thyroid nodules are palpable in 5% of subjects (1,2), but are detectable by thyroid ultrasound in up to 50% of the general population (3-4).

Cytological examination of material obtained by fine needle aspiration (FNA), due to its high sensitivity and specificity, is the best single test for differentiating malignant from benign thyroid lesions (5). The major limitations of FNA cytology are the occurrence of nondiagnostic (10-15%) and indeterminate (10-20 %) cytology (6-7).

The newly developed ultrasound elastography (US elastography) has been applied to study the stiffness/elasticity of nodules, with the purpose of differentiating malignant from benign lesions. As for thyroid cancer, a low elasticity on US elastography showed a high predictive value in the assessment of malignancy (8-9). The reliability of US elastography was confirmed by several authors and recently reviewed in a meta-analysis (10). Interestingly, US elastography maintains its high predictive value in thyroid nodules with indeterminate cytology in our (11) and other series (12-16). Hence, US elastography can be considered an additional diagnostic tool for the management of indeterminate thyroid lesions (2-3). The results obtained with real time US elastography were confirmed by quantitative elastographic techniques, such as strain index, acoustic radiation force impulse and supersonic shear wave (17-18).

The tissue proprieties that link stiffness to cancer in thyroid nodules are unknown. Theoretically, an increased cell number and/or fibrosis could account for nodule stiffness. An increased expression of molecules involved in cell to cell and cell to matrix adhesion as well as in fibrosis has been described in thyroid neoplasia. In addition, some of them, such as Gal-3 (19-23) and HBME-1 (24-26) have also been employed as cytochemical tumor markers. To validate real-time US elastography as a robust new technique for the assessment of malignancy in thyroid nodules we decided to compare real time qualitative with quantitative US elastography in a series of patients and to analyze tissue proprieties in surgical samples that could correlate with nodule stiffness such as cell number, microvessel density, degree of fibrosis and expression of Gal-3 and FN-1.

Patients and Methods

Patients

In the period January to March 2012 patients with 1 or 2 nodules in the absence of confounding factors such as thyroiditis, multinodularity with coalescent nodules and macrocalcifications underwent US elastography. Among them 112 patients (mean age 44 + 13 yr; range 8-74; 78 females and 34 males) in whom surgery was indicated for Thy 3 cytology (n=67), Thy 4-5 cytology (n= 47) or large goiter in the presence of Thy 2 cytology (n= 1) and suspicious US features (1,2) were selected for this study. Three patients had two nodules with Thy 3 cytology. Thus, a total of 115 nodules were included in the study. Nodular volume (mean +SD) was 4.6 + 9.76 ml. Patients gave their consent to participate in the study allowing molecular analysis of biological material. All patients were euthyroid in the absence of circulating thyroid autoantibodies and had undetectable serum calcitonin

measured with immunoradiometric assay (CIS BIO International, France, normal values <10 ng/mL).

Fine needle aspiration cytology

FNA was performed under US guidance using a 23 gauge needle attached to a 10 mL syringe. The material was air-dried, stained with Papanicolaou and Giemsa and interpreted by two experienced cytologists (DG, MI). The adequacy of aspirates was defined according to the guidelines of the Papanicolaou Society (27). Results of cytology were reported according to the Italian Consensus (28).

Histological diagnosis and morphological features

Histological diagnoses were made with standard procedure (hematoxylin/eosin), according to the WHO 2004 system (29) and confirmed independently, in a blinded fashion by three pathologists (A.P., L.T., and F.B.). Tumor fibrosis was expressed as the percentage of dense connective tissue with respect to the tumor cell-occupied area in the whole nodule (2 to 5 slides) and expressed both as mean value ± SD and median with interquartile range (IQR). To evalutate the number of cells, the slides were observed under a standard Nikon TS100F microscope (Nikon Instruments, Florence, Italy) connected to a digital video system. Using a 40×magnification lens, three fields representative of the whole nodule were sampled randomly and photographed using an MMI GmbH digital microphotography system (Nikon Instruments). Cells were counted by an image analysis using the Nis Elements AR software (Nikon Instruments) and reported as mean ± SD.

To evaluate tumor microvessel density, tissue sections were immunostained with an anti-CD34 primary antibody using an automated Benchmark IHC staining system (Ventana,

Tucson, Arizona, USA). The immunostained slides were observed under a 40x magnification lens with a standard microscope connected to a digital video system, as described above. Three representative fields with the highest vascularity were chosen for each sample and photographed as previously described. Results were reported as the area occupied by the microvessel (μm^2/field, mean value ± SD). AP, FB, LT who performed cytology, pathology, and evaluation of cell number, microvessel density and fibrosis were unaware of the US elastography data.

RNA purification and complementary DNA synthesis

After standard deparaffinization, formalin-fixed and paraffin-embedded (FFPE) thyroid tissue sections (5 μm) were enriched by manual microdissection. Then, RNA was extracted and purified from the FFPE tissue sections using the Qiagen RNeasy FFPE kit (GmbH, Hilden, Germany). RNA integrity was assessed by spectrophotometry (NanoDrop ND-1000 Technologies, Wilmington, DE, USA).

Semiquantitative real-time reverse-transcription polymerase chain reaction (PCR)

Gal-3 and FN-1 mRNA quantification was performed using the real time quantitative PCR Rotor Gene Sybr Green PCR kit (Qiagen) on a Rotor Gene 6000 (Qiagen) instrument. Quanti tect primer assays (Qiagen) were used for Gal-3 (NM_001177388, NM_002306, NM_194327), FN-1 (NM_002026, NM_212474, NM_212475, NM_212476, NM_212478, NM_212482) and beta-actin (NM_001101) as an internal control. Pooled normal thyroid tissues were used as external control. The comparative threshold cycle (Ct) method, defined as $2^{-\Delta\Delta Ct}$, was used for calculation of fold amplification of each sample *versus* external control. Each experiment was evaluated with three PCR reactions. Data are presented as the mean value ± SD. Gal-3 and FN-1 mRNA expression of each sample was normalized by

calculating the z score obtained by subtracting the population mean and dividing by the standard deviation. The converted z scores were then aggregated into one large set, identifying two different categories: 'low expression' (negative z score) and 'high expression' (positive z score). RG, NB, who measured expression of FN-1 and Gal-3 were unaware of the US elastography data as well as the cytology and pathology data.

Thyroid US elastography

Thyroid US elastography was performed using a real-time instrument (Esaote SPA, My Lab 70) with a linear transducer (8-13 MHz). The qualitative analysis of US elastography was performed using the methodology previously described (9,11). In nodules with high elasticity (HiEl) the green color was clearly dominant and classified as likely benign; in nodules with intermediate elasticity the pattern of color distribution was inhomogeneous with both green and blue color represented and classified as suspicious. In nodules with very low elasticity the blue color was clearly predominant and classified as likely malignant. Nodules with intermediate and low elasticity were grouped and classified as nodules with low elasticity (LoEl).

For the quantitative analysis the operator used had an electronic box, which included the selected nodule and an adequate amount of surrounding parenchyma. Two regions of interest, one corresponding to the nodule and one to the softest area of normal parenchyma were identified on elastogram. The elastic ratio (ER) between the strain of the nodule and the surrounding thyroid parenchyma was calculated automatically by the software (30). During the study ER, became available and we decided, as a secondary endpoint, to compare the results of the two techniques. Unfortunately, the majority of patients had already been

surgically treated and only 24 nodules were available for this comparison. US elastography was performed by TR, MS ad VL before FNA. *In vivo* examination was performed by 2 examiners. Static and moving images were also recorded to be reviewed by the third examiner. The agreement on the US elastography scoring among the three examiners was > 90%.

Statistical analysis

Proportions and frequencies in the group of patients were compared using the $\chi 2$ test and the Fischer exact test, when appropriate. The Kolmogorov-Smirnov test was employed to test the normality of data distribution. Student's t-test and Mann-Whitney U test were US elastography had to detect difference between groups for normal and skewed variables, respectively. A p-value less than or equal to 0.05 was considered statistically significant. Statistical analyses were performed using the SPSS for Windows 10.0 computer software (SPSS Inc., Chicago, IL). ROC curve analyses were performed to identify the ER cut-off that better discriminated between carcinomas and benign nodules in term of sensitivity and specificity (i.e., highest Youden index).

Results

1. Cytology and Histology

Among the 67 nodules with Thy 3 cytology, 20 (31%) were papillary carcinomas on histology (14 follicular variant, 6 classic variant) and 1 was a minimally invasive follicular thyroid carcinoma. The remaining 46 (69%) were benign: 37 were follicular adenomas, 2

hyperplastic nodules and 7 follicular adenomas with foci (<5 mm) of papillary carcinoma (Table 1).

Among the 47 nodules with Thy 4-5 cytology, 46 (98%) were papillary thyroid carcinomas (29 classic variant, 10 follicular variant and 7 tall cell variant); 1 nodule was hyperplastic.

The large nodule with Thy 2 cytology was a follicular variant of papillary carcinoma on histology (Table 1).

2. US elastography

HiEl at real time US elastography was found in 49 cases, 46 benign lesions and 3 carcinomas; LoEl was observed in 66 cases, 65 carcinomas and one benign nodule (Fig. 1). Thus, low elasticity was highly predictive of malignancy ($p<0.0001$). The ER was 1.90 (1.18-2.77) (median and IQR) in 14 nodules with LoEl and 1.01-(0.91-1.10) in 10 nodules with HiEl ($p=0.002$). The ER cut-off of 1.1 identified carcinomas with a sensitivity of 86 % (12/14) and benign nodules with a specificity of 90% (9/10), the negative predictive value was 82%, the positive predictive value 92% (Fig. 2).

3. Correlation between US elastography and cellularity, microvessel density, degree of fibrosis and expression of Gal-3 and FN-1

Cell number did not correlate with elasticity: 334 (289-408) (median and IQR) cells/field in nodules with HiEl and 308.5 (255-366.5) cells/field in nodules with LoEl ($p=0.12$). On the other hand, microvessel density inversely correlated with elasticity: 168.2 (125.7-217) μm^2/field (median and IQR) in nodules with HiEl and 108.6 (92.4-158.5) μm^2/field in those with LoEl ($p<0.001$).

The degree of fibrosis inversely correlated with elasticity: 5 (0-10) (median and IQR) in nodules with HiEl and 10 (0-30) in nodules with LoEl ($p=0.009$).

Among the 49 nodules with HiEl, 2 had high and 47 low expression of Gal-3, while out of the 66 nodules with LoEl, 37 had high and 29 low expression of Gal-3 ($p<0.001$). All the 49 nodules with HiEl had low expression of FN-1, while of the 66 nodules with LoEl 27 had high and 39 low expression of FN-1 ($p<0.001$) (Table 2). Thus, with regard to the finding of LoEl, low expression of Gal-3 had a negative predictive value (NPV) of 95.9%, while high expression of Gal-3 had a positive predictive value (PPV) of 94.8 %. Low expression of FN-1 had a NPV of 100%, while high expression of FN-1 had a PPV of 40.9%.

4. Correlation between histology and cellularity, microvessel density, degree of fibrosis and expression of Gal-3 and FN-1

While cell number did not differ between benign nodules (333.5 [284-408] cells/field), (median and IQR) ($p=0.15$) and carcinomas (309 [256-371] cells/field), microvessel density was higher in benign nodules (173.1 [129-223.6] μm^2/field), (median and IQR) than in carcinomas (108.8 [92.4-157.6] μm^2/field), ($p<0.001$). The degree of fibrosis was higher in carcinomas 10 (0-30) (median and IQR) than in nodules with benign histology 5 (0-10) ($p=0.02$). Among the 47 benign nodules,1 had high and 46 low expression of Gal-3, while out of the 68 carcinomas 38 had high and 30 low expression of Gal-3, ($p<0.001$). All the 47 benign nodules had low expression of FN-1, while among 68 carcinomas, 27 had high and 41 low expression of FN-1 ($p<0.001$) (Table 3). Fibrosis was 20 (3-40) (median and IQR) in nodules with high expression of Gal-3, and 5 (0-10) in those with low expression of Gal-3 ($p<0.001$). Fibrosis was 20 (3-40) in nodules with high expression of FN-1, and 5 (0-12.5) in those with low expression of FN-1 ($p=0.004$) (data not shown).Thus, with regard to the histological diagnosis of carcinoma, low expression of Gal-3 had a NPV of 97.8%, while

high expression of Gal-3 had a PPV of 55.8 %. Low expression of FN-1 had a NPV of 100%, while high expression of FN-1 had a PPV of 39.7%.

5. *US elastography, cellularity, microvessel density and degree of fibrosis in the classic and the follicular variant of papillary thyroid carcinoma and in follicular adenoma*

Out of the 35 classic variant of papillary thyroid carcinoma, 1 had HiEl, and 34 had LoEl, while out of the 25 follicular variant, 2 had HiEl and 23 LoEl ($p<0.001$). In contrast, all the 37 follicular adenomas had HiEl. Cell number was 334 (289-408) cells/field, (median and IQR) in follicular adenomas, 336 (244-474) in the follicular variant of papillary thyroid carcinoma, 309 (256-349) in the classic variant ($p=0.15$). The microvessel density was 182.5 (148.7-230.2) μm^2/field (median and IQR) in follicular adenomas, 115.5 (92.4-200.4) μm^2/field in the follicular variant of papillary thyroid carcinoma, and 107.7 (92.6-105.5) μm^2/field in the classic variant ($p=0.001$). The degree of fibrosis was 5 (0-10) (median and IQR) in follicular adenomas, 5 (0-20) in the follicular variant, and 17.5 (2-30) in the classic variant of papillary carcinoma ($p=0.01$). In addition, high expression of both Gal-3 and FN-1 was found more often in the classic variant than in the follicular variant of papillary thyroid carcinomas and almost never in the follicular adenomas with only 1 out of 37 showing high expression of Gal-3 (Table 4).

Discussion

Real time US elastography has been shown to be a useful diagnostic tool in the management of thyroid nodules, with high elasticity having a high negative predictive value for thyroid carcinoma even in indeterminate nodules (9,11). The results obtained by real time

elastography were confirmed by methods providing an objective measurement of tissue stiffness such as strain index, acoustic radiation force impulse and supersonic shear wave (17-18).

The aim of this study was to compare the qualitative real time with quantitative US elastography and correlate US elastography findings with tissue properties associated with stiffness/elasticity of thyroid nodules. An optimal correlation between nodule stiffness and thyroid cancer was confirmed. The elasticity was measured both by qualitative real time and quantitative US elastography and data obtained by the two methods were highly correlated, thus validating the qualitative measurements and strengthening the value of this technique. The reason why tissue stiffness is correlated with malignancy is unknown. We hypothesized that the number of cells, the microvessel density and the degree of fibrosis could be the factors involved in the stiffness/ elasticity of thyroid nodules.

Stiffness did not correlate with cell number, while it was inversely correlated with the microvessel density, and positively associated with fibrosis. A similar cell number in benign adenomas compared to papillary thyroid cancer is not surprising given that both lesions show histological features with high cellularity and low colloid content. On the other hand, the inverse relationship with the microvessel density was unexpected. Indeed, malignant lesions are supposedly characterized by high vascularization. The number of vessels, but not the area of vascular surface, was found to be higher in benign lesions compared to carcinoma (31). On the other hand, tumor microvessel density has been reported to be directly associated with recurrence in differentiated thyroid cancer (32). Proietti at al. found that follicular adenomas had more extensive intratumoral hemorrhage and peripheral vascularization (33). Results

obtained by *in vivo* determination of vascularization with color Doppler US (2,3) are contradictory and not suggestive for a difference between benign and malignant thyroid nodules (34). Our results suggest that malignant nodules are characterized by a higher fibrosis/microvessel density ratio as compared to benign lesions.

The activation of the fibrotic process has been described in cancers occurring in several tissues and in thyroid cancers as well (35,36). The development of fibrosis is related to a aberrant activation of myofibroblasts that play a crucial role in tumor progression (38). In several tissues, an increased risk of cancer progression has been linked to the stromal collagen content. Several factors are involved in this process, including transforming growth factors, which induce differentiation of fibroblasts to myofibroblasts (38). In the present study, the degree of fibrosis was strictly correlated with the stiffness at US elastography. In addition, both stiffness and fibrosis were correlated with malignancy. Therefore, these results highlight that the higher expression of fibrosis in thyroid cancer is the link between malignancy and stiffness on US elastography, as well as hardness on physical examination (1,3).

After the finding of the role of fibrosis, evaluated by histology, we investigated the correlation between stiffness and some molecules involved in fibrosis and in the processes of cell-to-cell and cell-to-matrix adhesion. Low elasticity was correlated with a high expression of Gal-3 and FN-1. In several studies, an increased expression of Gal-3 has been related to malignant transformation, tumor progression and metastasis (21-24). In addition, Gal-3 has been proposed as a thyroid tumor marker, because its expression has been found to be increased in fine needle aspiration material as well as in histological samples of thyroid carcinomas (22,25). FN-1, an extracellular matrix protein produced by fibroblasts, has been

associated with malignancy (35-37) in several tissues. A high expression of FN-1 in thyroid carcinomas has been reported by several, but not all series (38-40). FN-1 is also expressed in fibrous tissue and basement membrane of goiters (37). In our series of thyroid nodules, a high expression of both Gal-3 and FN-1 was associated with fibrosis and malignancy. Interestingly, the NPV for nodule stiffness of the low expression of both Gal-3 and FN-1 was higher than the PPV of high expression of both molecules, in agreement with the observation that the NPV for malignancy is much higher than its PPV of high expression of both molecules (9).

In summary, our data indicate that, compared to benign nodules, thyroid carcinomas have a similar number of cells, lower microvessel density and higher degree of fibrosis. When we examined the results obtained in nodules grouped according to the histological subtype, we observed that the microvessel density was lower in the classic variant, intermediate in the follicular variant of papillary carcinomas, and higher in follicular adenomas. In contrast, the degree of fibrosis, as well the expression of Gal-3 and FN-1 were the highest in the classic variant, intermediate in the follicular variant, and lowest in the follicular adenomas.

In conclusion, our results confirm that nodule stiffness on US elastography is highly indicative of malignancy and show that real time qualitative elastography correlates well with quantitative elastography. We have also shown with a morphological approach that stiffness in thyroid nodules is inversely correlated with the microvessel density and directly correlated with fibrosis. Higher expression of molecules involved in the processes of fibrosis and cell-to-cell and cell-to-matrix adhesion such as Gal-3 and FN-1 are related to nodule stiffness and malignancy. These features characterize the classic variant vs the follicular variant of

papillary thyroid carcinoma. More studies are needed to better understand the processes that cause stiffness in thyroid cancer

References

1. Cooper DS, Doherty GM, Haugen BR, Kloos RT, Lee SL, Mandel SJ, Mazzaferri EL, McIver B, Pacini F, Schlumberger M, Sherman SI, Steward DL, Tuttle RM 2009 American Thyroid Association (ATA) Guidelines Taskforce on Thyroid Nodules and Differentiated Thyroid Cancer. Revised American Thyroid Association management guidelines for patients with thyroid nodules and differentiated thyroid cancer. Thyroid **19**:1167-214.

2. Gharib H, Papini E, Garber JR, Duick DS Harrell RM, Hegedus L, Paschke R, Valcavi R, Vitti P 2016 The AACE/ACE/AME Task Force on Thyroid Nodule. American Association of Clinical Endocrinologists, American College of Endocrinology, and Associazione Medici Endocrinologi, Guidelines for Clinical Practice for the Diagnosis and Management of Thyroid Nodules. Endocr Pract. 22: 622-39.

3. Gharib H, Papini E, Paschke R **2008** Thyroid nodules: a review of current guidelines, practices, and prospects. Eur J Endocrinol.**159**: 493-505.

4.Aghini-Lombardi F, Antonangeli L, Martino E, Vitti P, Maccherini D, Leoli F, Rago T, Grasso L, Valeriano R, Balestrieri A, Pinchera A 1999 The spectrum of thyroid disorders in an iodine-deficient community: the Pescopagano survey. J Clin Endocrinol Metab **84**: 561-566.

5. Castro MR, Gharib H 2003 Thyroid fine-needle aspiration biopsy: progress, practice, and pitfalls. Endocr Pract **9**: 128–136.

6. Rago T, Di Coscio G, Basolo F, Scutari M, Elisei R, Berti P, Miccoli P, Romani R, Faviana P, Pinchera A, Vitti P 2007 Combined clinical, thyroid ultrasound and cytological features help to predict thyroid malignancy in follicular and Hürthle cell thyroid lesions: results from a series of 505 consecutive patients. Clin Endocrinol **66**: 13-20.

7. Gharib H, Papini E 2007 Thyroid nodules: clinical importance, assessment, and treatment. Endocrinol Metab Clin North A **36**: 707-735.

8. Lyshchik A, Higashi T, Asato R, Tanaka S, Ito J, Mai J, Pellot-Barakat C, Insana MF, Brill AB, Saga T, Hiraoka M, Togashi K 2005 Thyroid Gland tumor diagnosis at US Elastography. Radiology **237**:202–211

9. T. Rago T, ScutarI M, Santini F, Loiacono V, Piaggi P, Di Coscio G, Basolo F, Berti AP, Pinchera, A, Vitti P 2010 Real- time elastosonography: US Elastographyful tool for refining the presurgical diagnosis in thyroid nodules with indeterminate or nondiagnostic cytology. J Clin Endocrinol Metab 95:5274-80.

10. Bojunga J, Herrmann E, Meyer G, Weber S, Zeuzem S, Friedrich-Rust M 2010 Real-time Elastography for the differentiation of benign and malignant thyroid nodules: a meta-analysis. Thyroid **20**:1145-50.

11. Rago T, Santini F, Scutari M, Pinchera A, Vitti P. 2007 Elastosonography: new developments in ultrasound for predicting malignancy in thyroid nodules. J Clin Endocrinol Metab **9**: 2917-2922.

12. Asteria C, Giovanardi A, Pizzocaro A, Cozzaglio L, Morabito A, Somalvico F, Zoppo A 2008 US-elastosonography in the differential diagnosis of benign and malignant thyroid nodules. Thyroid 18: 523-531.

13. Hong Y, Liu X, Li Z, Zhang X, Chen M, Luo Z 2009 Real-time ultrasound Elastography in the differential diagnosis of benign and malignant thyroid nodules. J Ultrasound Med **287**: 861-867.

14**.** Russ G, Royer B, Bigorgne C, Rouxel A, Bienvenu-Perrard M, Leenhardt L 2013 Prospective evaluation of thyroid imaging reporting and data system on 4550 nodules with and without Elastography. Eur J Endocrinol **168**: 649–655.

15. Trimboli P, Guglielmi R, Monti S, Misischi I, Graziano F, Nasrollah N, Amendola S, Morgante SN, Deiana MG, Valabrega S, Toscano V, Papini E 2012 Ultrasound sensitivity for thyroid malignancy is increased by real-time Elastography: a prospective multicenter study. J Clin Endocrinol Metab **97**: 4524-30.

16. Magri F, Chytiris S, Capelli V, Gaiti M, Zerbini F, Carrara R, Malovini A, Rotondi M, Bellazzi R, Chiovato L 2013 Comparison of elastographic strain index and thyroid fine-needle aspiration cytology in 631 thyroid nodules. J Clin Endocrinol Metab **12**: 4790-7.

17. Liang XN, Guo RJ, Li S, Zheng ZM, Liang HD. 2014 Binary logistic regression analysis of solid thyroid nodules imaged by high-frequency ultrasonography, acoustic radiation force impulse, and contrast-enhanced ultrasonography. Eur Rev Med Pharmacol Sci **18**: 3601-10.

18. Sebag F, Vaillant-Lombard J, Berbis J, Griset V, Henry JF, Petit P, Oliver C 2010 Shear wave Elastography: a new ultrasound imaging mode for the differential diagnosis of benign and malignant thyroid nodules. J Clin Endocrinol Metab. 95:5281–5288.

19. Kim ES, Lim DJ, Lee K, Jung CK, Bae JS, Jung SL, Baek KH, Lee JM, Moon SD, Kang MI, Cha BY, Lee KW, Son HY 2012 Absence of galectin-3 immunostaining in fine-needle aspiration cytology specimens from papillary thyroid carcinoma is associated with favorable pathological indices. Thyroid **22**:1244-5.

20. Savin S, Cvejic D, Isic T, Paunovic I, Tatic S, Havelka M 2008 Thyroid peroxidase and galectin-3 immunostaining in differentiated thyroid carcinoma with clinicopathologic correlation. Hum Pathol 39: 1656-63.

21. Kawachi K, Matsushita Y, Yonezawa S, Nakano S, Shirao K, Natsugoe S, Sueyoshi K, Aikou T, Sato E. 2000 Galectin-3 expression in various thyroid neoplasms and its possible role in metastasis formation. Hum Pathol 31:428-33.

22. Torregrossa L, Faviana P, Camacci T, Materazzi G, Berti P, Minuto M, Elisei R, Vitti P, Miccoli P, Basolo F 2007 Galectin-3 is highly expressed in nonencapsulated papillary thyroid carcinoma but weakly expressed in encapsulated type; comparison with Hector Battifora mesothelial cell 1 immunoreactivity. Hum Pathol **38**: 1482-8.

23. Giannini R, Faviana P, Cavinato T, Elisei R, Pacini F, Berti P, Fontanini G, Ugolini C, Camacci T, De Ieso K, Miccoli P, Pinchera A, Basolo F 2003 Galectin-3 and oncofetal-fibronectin expression in thyroid neoplasia as assessed by reverse transcription-polymerase chain reaction and immunochemistry in cytologic and pathologic specimens. Thyroid **13**: 765-70.

24. Liu YY, Morreau H, Kievit J, Romijn JA, Carrasco N, Smit JW 2008 Combined immunostaining with galectin-3, fibronectin-1, CITED-1, Hector Battifora mesothelial-1, cytokeratin-19, peroxisome proliferator-activated receptor-{gamma}, and sodium/iodide symporter antibodies for the differential diagnosis of non-medullary thyroid carcinoma. Eur J Endocrinol **158**: 375-84

25. de Matos LL, Del Giglio AB, Matsubayashi CO, de Lima Farah M, Del Giglio A, da Silva Pinhal MA 2012 Expression of CK-19, galectin-3 and HBME-1 in the differentiation of thyroid lesions: systematic review and diagnostic meta-analysis. Diagn Pathol. 13: 7-97.

26. Prasad ML, Pellegata NS, Huang Y, Nagaraja HN, de la Chapelle A, Kloos RT 2005 Galectin-3, fibronectin-1, CITED-1, HBME1 and cytokeratin-19 immunohistochemistry is US Elastographyful for the differential diagnosis of thyroid tumors. Mod Pathol. 18: 48-57.

27. Guidelines of the Papanicolaou Society of Cytopathology for the Examination of Fine-Needle Aspiration Specimens from Thyroid Nodules 1996 The Papanicolaou Society of Cytopathology Task Force on Standards of Practice. Mod Pathol **9**: 710–715.

28. Nardi F, Basolo F, Crescenzi A, Fadda G, Frasoldati A, Orlandi F, Palombini L, Papini E, Zini M, Pontecorvi A, Vitti 2014 Italian consensus for the classification and reporting of thyroid cytology. J Endocrinol Invest **37**: 593-9.

29. DeLellis RA. Loyd RV, Heitz PU, Eng C. World Health Organization Classification of Tumors. Pathology and genetics of tumors of endocrine organs. Lyon: IARC Press, 2004.

30. MyLab ElaXto option. Rev. 08, 2014; 26.

31. Rzeszutko M, Rzeszutko W, Dziegiel P 2004 The morphological analysis of vasculature in thyroid tumours: immunoexpression of CD34 antigen. Folia Histochem Cytobiol. **42**: 235-4

32. Dhar DK, Kubota H, Kotoh T, Tabara H, Watanabe R, Tachibana M, Kohno H, Nagasue N 1999 Prognostic significance of perioperative blood transfusions in resectable thoracic esophageal cancer Am J Gastroenterol **94**:757-65.

33. Proietti A, Sartori C, Borrelli N, Giannini R, Materazzi G, Leocata P, Elisei R, Vitti P, Miccoli P, Basolo F 2013 Follicular-derived neoplasms: morphometric and genetic differences. J Endocrinol Invest **36**: 1055-61.

34. Moon HJ, Kwak JY, Kim MJ, Son EJ, Kim EK 2010 Can vascularity at power Doppler US help predict thyroid malignancy? Radiology **255**: 260-9.

35. O'Connor JW, Gomez EW 2014 Biomechanics of TGFβ-induced epithelial-mesenchymal transition: implications for fibrosis and cancer. Clin Transl Med **15:** 3-23.

36. Wasenius VM, Hemmer S, Kettunen E, Knuutila S, Franssila K, Joensuu H 2003 Hepatocyte growth factor receptor, matrix metalloproteinase-11, tissue inhibitor of metalloproteinase-1, and fibronectin are up-regulated in papillary thyroid carcinoma: a cDNA and tissue microarray study. Clin Cancer Res 9: 68-75.

37. Bhowmick NA, Neilson EG, Moses HL. 2004 Stromal fibroblasts in cancer initiation and progression. Nature **432**: 332-7.

38. Ryu S, Jimi S, Takebayashi S 1997 Thyroid carcinoma distinctively expresses intracellular fibronectin in vivo. Cancer Lett **12**: 189-9.)

39. Takano T, Matsuzuka F, Sumizaki H, Kuma K, Amino N 1997 Rapid detection of specific messenger RNAs in thyroid carcinomas by reverse transcription-PCR with

degenerate primers: specific expression of oncofetal fibronectin messenger RNA in papillary carcinoma. Cancer Res **57**: 3792-7.

40. Huang Y, Prasad M, Lemon WJ, Hampel H, Wright FA, Kornacker K, LiVolsi V, Frankel W, Kloos RT, Eng C, Pellegata NS, de la Chapelle A 2001Gene expression in papillary thyroid carcinoma reveals highly consistent profiles. Proc Natl Acad Sci USA **98**:15044-9.

This research did not receive any specific grant from any funding agency in the public, commercial or not-for-profit sector

Legend of Figures

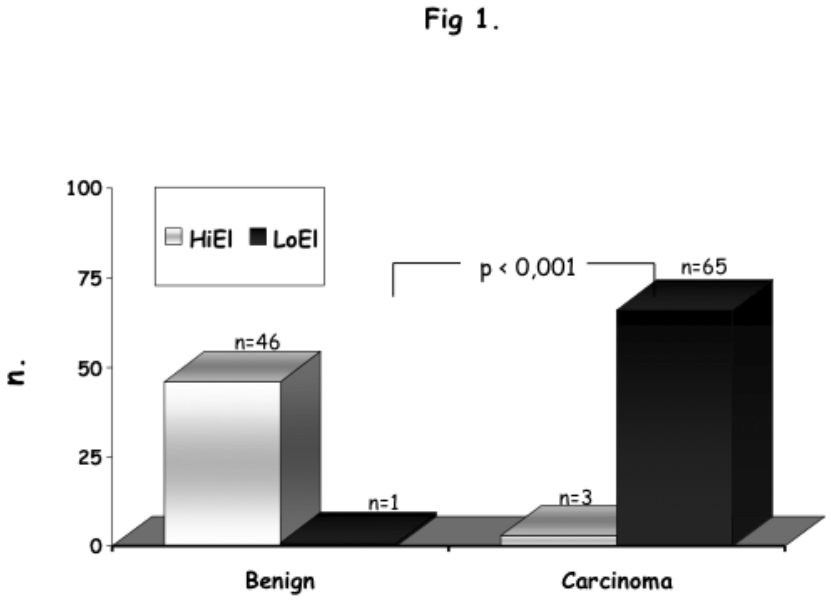

FIG. 1 Elasticity of thyroid nodule in relation to the final histology of benign lesion (BN) or carcinoma (CA). HiEl: open □ square ( ); LoEl: closed ■ square ( )

Fig 2.

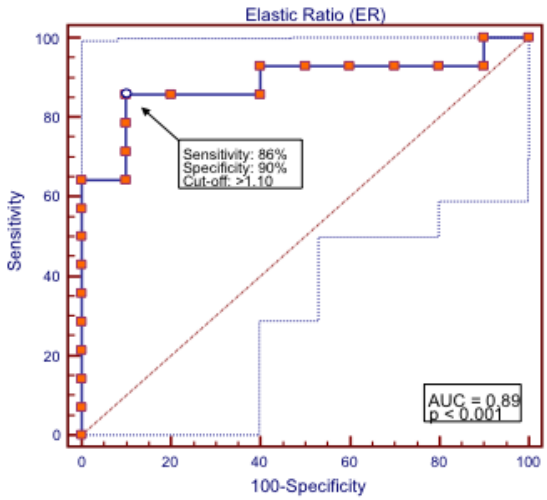

FIG. 2.ROC curve describing sensitivity and specificity of quantitative USE. The elastic ratio (ER) was 1.90 (1.18-2.77) (median and IQR) in 14 nodules with LoEl and 1.01-(0.91-1.10) in 10 nodules with HiEl (p=0.002). The ER cut-off of 1.1 identified carcinomas with a sensitivity of 86 % (12/14) and benign nodules with a specificity of 90% (9/10), with a negative predictive value of 82% and a positive predictive value of 92%

TABLE 1.Cytology and Histology in 115 thyroid nodules

Hystology	**Carcinoma (N= 68)**					**Benign (N=47)**		
Cythology	CVPC	FVPC	TCPC	MIFC		FA	HN	AFP
Thy 2 No= 1	/	1	/	/		/	0	/
Thy 3 No= 67	6	14	/	1		37	2	7
Thy 4-5 No = 47	29	10	7	/		/	1	/
Total	35	25	7	1		37	3	7

Classic variant of papillary carcinoma (CVPC), follicular variant (FVPC), tall cell variant (TCPC); minimally invasive follicular carcinoma (MIFC); follicular adenoma (FA), hyperplastic nodule (HN); adenoma with foci of papillary carcinoma (AFPC)

TABLE 2. Elasticity at US elastography in relationship with cellularity, microvessel density, degree of fibrosis and expression of Gal-3 and FN-1.

	HiEl (N= 49)	**LoEl (N=66)**	**p**
Cell number /field (median and IQR)	334 (289-408)	308.5 (255-366.5)	0.12
Microvessel density (μm^2/field) (median and IQR	168.2 (125.7-217)	108.6 (92.4-158.5)	<0.001
Degree of fibrosis (%) (median and IQR)	5 (0-10)	10 (0-30)	0.009
Gal-3* High Low	 2 47	 37 29	<0.001
FN-1** High Low	 0 49	 27 39	<0.001

*NPV 95.9%; PPV: 94.8 %
** NPV 100% : PPV: 40.9%

Low elasticity of thyroid nodules at ultrasound elastography is correlated with malignancy, degree of fibrosis and high expression of galectin-3 and fibronectin-1. (doi: 10.1089/thy.2016.0341)
This paper has been peer-reviewed and accepted for publication, but has yet to undergo copyediting and proof correction. The final published version may differ from this proof.

TABLE 3. Histological diagnosis of benign nodule (BN) or carcinoma (CA) in relationship with cellularity, microvessel density, degree of fibrosis, expression of Gal-3 and FN-1.

	BN (N=47)	**CA (N= 68)**	**p**
Cell number /field (median and IQR)	333.5 (284-408)	309 (256-371)	0.15
Microvessel density (μm^2/field) (median and IQR)	173.1 (129-223.6)	108.8 (92.4-157.6)	<0.001
Degree of fibrosis (%) (median and IQR)	5 (0-10)	10 (0-30)	0.02
Gal-3*			
High	1	38	<0.001
Low	46	30	
FN-1**			
High	0	27	<0.001
Low	47	41	

Benign Nodule (BN); Carcinoma (CA)

*NPV 97.8%; PPV: 55.8 %
** NPV 100% : PPV: 39.7 %

TABLE 4. Elasticity at US elastography, cellularity, microvessel density and fibrosis in classic and follicular variant of papillary thyroid carcinoma and in follicular adenoma.

	FAPC (N= 37)	**FVPC (N= 25)**	**CVPC (N= 35)**	**p**
USE HiEl LoEl	 37 0	 2 23	 1 34	 <0.001
ER* (n=16)	1.16 (n=3)	1.50 (n=6)	2.19 (n=7)	0.130
Cell number /field (median and IQR)	334 (289-408)	336 (244-474)	309 (256-349)	0.15
Microvessel density(μm^2/field) (median and IQR)	182.5 (148.7-230.2)	115.5 (92.4-2004)	107.7 (92.6-150.5)	0.001
Degree of fibrosis (%) (median and IQR)	5 (0-10)	5 (0-20)	17.5 (2-30)	0.01
Gal-3 High Low	 1 36	 13 12	 22 12	 <0.001
FN-1 High Low	 0 37	 7 18	 16 18	 <0.001

Follicular adenoma (FA), follicular variant of Papillary carcinoma (FVPC), classic variant of Papillary carcinoma (CVPC);
*ER was measured in a total number of 16 nodules of this subgroup. The number of nodule in each histological category is reported in parenthesis.